New Thermal and Trajectory Model for High-Altitude Balloons

Leland A. Carlson* and Walter J. Horn†
Texas A&M University, College Station, Texas

A new computer model for the prediction of the trajectory and thermal behavior of high-altitude balloons has been developed. In accord with flight data, the model permits radiative emission and absorption of the lifting gas and daytime gas temperatures above that of the balloon film. It also includes ballasting, venting, and valving. Predictions obtained with the model are compared with flight data and newly discovered features are discussed.

Nomenclature

A = cross-sectional area of sphere with volume equivalent to the balloon
c_f = specific heat of the balloon film
c_{pg} = specific heat of the balloon gas
C_D = coefficient of drag
CH_{fa} = convective heat-transfer coefficient between the balloon film and air
CH_{gf} = convective heat-transfer coefficient between the balloon film and gas
C_m = virtual mass coefficient
D = drag
$\dot{E}_g$ = balloon gas volume flow rate for expelling gas
$\dot{E}_v$ = balloon gas mass flow rate during valving
g = acceleration due to gravity
G = solar constant
Gr = Grashof number
m_f = mass of balloon film
m_g = mass of balloon gas
m_p = mass of payload
m_{tot} = total mass of balloon system
M_a = molecular weight of air
M_g = molecular weight of the balloon gas
Nu = Nusselt number
p_{a_l} = ambient air pressure at the base of a layer in an atmosphere model
p_g = pressure of the balloon gas
Pr_a = Prandtl number of air
$\dot{q}_f$ = net heat flux to balloon film
$\dot{q}_g$ = net heat flux to the balloon gas
r_w = reflectivity of the balloon film in the i.r. spectrum
r_e = Earth reflectivity (albedo)
r_{wsol} = reflectivity of the balloon film to solar radiation
R = universal gas constant
$\bar{R}$ = radius of a sphere with volume equivalent to the balloon
Re = Reynolds number
S = balloon surface area = $4.835976\ V^{2/3}$
t = time
T_a = ambient air temperature
T_{a_l} = ambient air temperature at the base of a layer in an atmosphere model
T_{BB} = blackball temperature
T_f = balloon film temperature
T_g = balloon gas temperature
V = balloon volume
z = balloon altitude
α_g = absorptivity of the balloon gas to solar radiation
α_{geff} = effective solar absorptivity of the balloon gas
α_w = absorptivity of the balloon film in the i.r. spectrum
α_{weff} = effective solar absorptivity of the balloon film
α_{wsol} = absorptivity of the balloon film in the solar spectrum
ϵ_g = emissivity of the balloon gas in the i.r. spectrum
ϵ_{geff} = effective i.r. emissivity of the balloon gas
ϵ_{int} = effective interchange i.r. emissivity
ϵ_w = emissivity of the balloon film in the i.r. spectrum
ϵ_{weff} = effective i.r. emissivity of the balloon film
μ_a = viscosity of the ambient air
ρ_a = air density
σ = Stefan-Boltzmann constant
τ_w = transmissivity of the balloon film in the i.r. spectrum
τ_{wsol} = transmissivity of the balloon film to solar radiation

Submitted Oct. 16, 1981; presented as Paper 81-1926 at the AIAA 7th Aerodynamic Decelerator and Balloon Technology Conference, San Diego, Calif., Oct. 21-23, 1981; revision received July 27, 1982.

*Professor, Aerospace Engineering Department. Member AIAA.
†Assistant Professor, Aerospace Engineering Department. Member AIAA.

Introduction

FOR the user, operator, and designer of high-altitude scientific balloons, the ability to accurately predict balloon trajectories and thermal behavior is important. For example, the successful design and execution of a scientific experiment frequently requires knowledge of the balloon rate of ascent, behavior at sunrise and sunset, and night and day float altitudes. For launch operations personnel, an accurate estimate of balloon performance behavior can greatly facilitate estimates of ballast requirements as well as balloon size selection. Likewise, the balloon designer needs accurate information concerning gas and film temperatures and rates of ascent/descent since these factors affect the balloon film stresses. In addition, if an anomaly or failure occurs, an accurate prediction method can assist in the determination of the cause and the development of remedial action.

By far the most significant work to date associated with the prediction of the performance of high-altitude balloons is that of Kreith and Kreider.[1,2] In a series of outstanding papers, they thoroughly discussed all pertinent phenomena, summarized existing knowledge, and developed an excellent model and computer program. Without a doubt, Ref. 1 was a benchmark effort, and thus it has served as a starting point for most subsequent investigations.

In their model, Kreith and Kreider included the effects of direct and reflected solar radiation, Earth and atmospheric infrared radiation, convection, and radiative emission. They also considered adiabatic heating and cooling, gas expulsion, valving, ballasting, and sunrise and sunset. In many cases, the resultant predictions agreed well with flight data.

In addition, based upon the radiative properties of helium, the Kreith-Kreider model assumed that the lifting gas was completely transparent to all radiation. Consequently, under float conditions the only mechanism heating or cooling the gas was convection between the gas and the film, which is proportional to the temperature difference $(T_f - T_g)$. Thus, in their model, the equilibrium gas temperature was equal to that of the film.

Several investigations have also been conducted to measure lifting gas and balloon film temperatures in flight. The first of these was a series of flights by Lucas and Hall[3-5] using 7080-m^3 balloons which floated at 24-26 km and measured film and gas temperatures during ascent, float, and through sunrise and sunset. Subsequently, in 1975 and 1976, the National Scientific Balloon Facility (NSBF) conducted a series of engineering test flights carefully designed to measure gas and film temperatures on larger balloons at higher altitudes. The equilibrium float temperatures measured on these flights, shown on Table 1, were quite surprising.

Specifically, while the night values supported the thermal model assumption that equilibrium wall and gas temperatures should be the same, the daytime measurements consistently showed a significant difference, with the lifting gas being warmer. In addition, since this phenomena only existed during daylight and, based upon the results of the RAD II and RAD III flights shown in Table 1, was sensitive to the amount of albedo radiation, it appeared that the gas temperature enhancement was primarily due to solar radiation.

However, since helium is undoubtedly transparent to solar radiation at the temperatures present in a balloon gas, this phenomenon is difficult to explain. One possibility is that during daylight, owing to uneven heating, the balloon film develops hot spots which through convection lead to a gas convection cell and a lifting gas supertemperature. Unfortunately, careful examination of the flight data did not reveal any film temperatures near or above the measured gas values, and thus this explanation does not seem likely. Obviously, the gas was somehow being heated by solar radiation, and the existing transparent gas thermal models were inadequate.

Consequently, Carlson[6] developed a new thermal model, based upon engineering radiation concepts, which permitted the lifting gas to emit and absorb radiation in both the solar and i.r. spectra. Unfortunately, owing to the lack of accurate film radiative property data, he was forced to simplify the model, to limit it to float conditions only, and to estimate film properties from flight data. Results obtained with this simplified model yielded excellent daytime values but consistently predicted night temperatures below those actually encountered in-flight. In addition, initial attempts using the Kreith-Kreider code to model these flights yielded discouraging results. Typically, when compared to the actual flights, they predicted too high ascent rates below the tropopause and too slow velocities above it.

Consequently, it was decided to develop a new trajectory and thermal analysis code incorporating the thermal model of Carlson, which would, from an engineering standpoint, be sufficiently accurate for flight prediction or analysis. Finally, it was decided to limit this initial code to zero-pressure balloons.

Thermal and Trajectory Model

Governing Equations

If it is assumed that the balloon trajectory problem can be treated two-dimensionally, (i.e., independent variables altitude z and time t), and that the film temperature T_f and gas temperature T_g are spatially averaged values, then the governing differential equations are as follows: the vertical force balance on the balloon—

$$(m_{\text{tot}} + C_m \rho_a V)\frac{d^2z}{dt^2} = g(\rho_a V - m_{\text{tot}}) - \tfrac{1}{2}\rho_a C_D \frac{dz}{dt}\left|\frac{dz}{dt}\right| A \tag{1}$$

the heat balance for the balloon film—

$$m_f c_f \frac{dT_f}{dt} = \dot{q}_f \tag{2}$$

the heat balance for the lifting gas—

$$m_g c_{pg}\frac{dT_g}{dt} = \dot{q}_g - \frac{gM_a m_g T_g}{T_a M_g}\frac{dz}{dt} \tag{3}$$

and the mass balance for the lifting gas—

$$\frac{dm_g}{dt} = \frac{p_g M_g}{RT_g}\dot{E}_g - \dot{E}_v \tag{4}$$

where

$$V = m_g R T_g / p_a M_g \tag{5}$$

$$m_{\text{tot}} = m_g + m_f + m_p \tag{6}$$

$$A = \pi \bar{R}^2 \tag{7}$$

$$S = 4\pi \bar{R}^2 \tag{8}$$

It should be noted that Eq. (3) not only accounts for heating effects on the balloon gas but also includes adiabatic expansion of the lifting gas. During ascent, the latter leads to a gas temperature that is cooler than the balloon wall temperature.

The forms for $\dot{q}_f$ and $\dot{q}_g$ are different from previous models owing to the incorporation of the new thermal model which permits gas emission and absorption. Following logic similar to that used in Ref. (6) and the engineering approach, as opposed to spectral, for radiative heat transfer, $\dot{q}_f$ and $\dot{q}_g$ can

Table 1 Equilibrium float temperatures from flight measurements

Flight		Day Altitude, km	Day Gas, °C	Day Film, °C	Night Altitude, km	Night Gas, °C	Night Film, °C
Lucas-Hall	Zero-pressure polyethylene, 7080 m^3	24.4	−32	−39	...	...	...
RAD I	Zero-pressure polyethylene, 56,634 m^3	33.5	−16.8	...	33.5	−47.4	...
RAD II[a]	Zero-pressure polyethylene, 14,160 m^3	29.7	−10	−36.5	25.9	−71	−71
RAD III	Zero-pressure polyethylene, 14,160 m^3	29.7	−22	−37.5	29.0	−47	−47

[a] Overcast skies; all others, clear skies.

be expressed as

$$\dot{q}_f = [G\alpha_{weff}(\tfrac{1}{4} + \tfrac{1}{2}r_\epsilon) + \epsilon_{int}\sigma(T_g^4 - T_f^4) + CH_{gf}(T_g - T_f) + CH_{fa}(T_a - T_f) - \epsilon_{weff}\sigma T_f^4 + \epsilon_{weff}\sigma T_{BB}^4]S \quad (9)$$

and

$$\dot{q}_g = [G\alpha_{geff}(1 + r_e) - \epsilon_{int}\sigma(T_g^4 - T_f^4) - CH_{gf}(T_g - T_f) - \epsilon_{geff}T_g^4 + \epsilon_{geff}\sigma T_{BB}^4]S \quad (10)$$

Since balloon film is semitransparent, any radiation to or from the balloon film will be partially transmitted, and then partially transmitted off the opposite wall an infinite number of times. Thus in Eqs. (9) and (10), α_{weff}, ϵ_{int}, ϵ_{weff}, α_{geff}, and ϵ_{geff} are effective coefficients which take into account this multiple-pass phenomena. Based upon Ref. 6, these quantities are defined in terms of the actual gas and wall radiative properties as

$$\alpha_{weff} = \alpha_w\left(1 + \frac{\tau_{wsol}(1-\alpha_g)}{1 - r_{wsol}(1-\alpha_g)}\right) \quad (11)$$

$$\epsilon_{int} = \frac{\epsilon_g \epsilon_w}{1 - r_w(1-\epsilon_g)} \quad (12)$$

$$\epsilon_{weff} = \epsilon_w\left(1 + \frac{\tau_w(1-\epsilon_g)}{1 - r_w(1-\epsilon_g)}\right) \quad (13)$$

$$\alpha_{geff} = \frac{\alpha_g \tau_{wsol}}{1 - r_{wsol}(1-\alpha_g)} \quad (14)$$

$$\epsilon_{geff} = \frac{\epsilon_g \tau_w}{1 - r_w(1-\epsilon_g)} \quad (15)$$

With proper input, initial values, and definitions, Eqs. (1-15) form a well-posed initial value problem for z, dz/dt, T_f, T_g, m_g, and volume.

Gas and Film Radiative Properties

Since the present model permits the gas to radiatively emit and absorb, estimates for α_g and ϵ_g must be made. Also, an explanation for the lifting gas radiative behavior needs to be postulated. An examination of helium reveals that it does contain several spectral lines in the solar spectrum.[8] However, these transitions are all between excited states; and at the temperatures present in balloons, the number of atoms in these states would be negligible. Consequently, it is highly unlikely that helium would directly absorb solar energy.

Another possibility is that the lifting gas contains a small amount of some contaminant which is intensely absorbing in the solar spectrum. This absorption would increase the energy and hence the temperature of the contaminant, and it would subsequently be rapidly transferred to the helium via particle-particle collisions. One possibility for this contaminant is water vapor, whose presence in even trace amounts is well known to drastically affect spectral measurements based on radiative processes.

One possible source of water vapor in balloons is in the air trapped inside it during manufacturing and packaging. If it is assumed that a balloon is assembled at 80% relative humidity, and 25°C, and packed with a 0.15875-cm layer of air trapped inside, then the amount of water contained in the balloon would range from 200 g for a small balloon to 2300 g for a large one. At a float altitude of 32 km and a gas temperature of about −15°C, the partial pressure of this water would range from 2 to 4 dyne/cm^2, and all of the water would be in vapor form and available for radiative absorption.

At this point, it should be pointed out that this water vapor explanation may be totally incorrect; and its verification depends upon future research. However, in the present model, exact knowledge of the contaminant is not required.

Now fortunately, the radiative properties of water vapor in the i.r. are well known and documented[7]; and based upon these, an equation suitable for estimating the gas emissivity can be found, i.e.,

$$\epsilon_g = 0.169\,(1.746 \times 10^{-6}\,T_g)^{0.8152} \quad (16)$$

where T_g is in Kelvin.

Based upon experimental data, float gas temperatures can range from 233 to 273K, which yields ϵ_g values from 0.00029 to 0.00033. These values of emissivity are very small; therefore their effect on balloon thermal behavior will be almost negligible. Furthermore, since the range of ϵ_g is very small over the entire range of balloon float gas temperatures, the value for T_g need only be approximated in Eq. (16) in order to obtain an accurate estimate of ϵ_g.

Unfortunately, the absorptivity radiative properties of water are not documented in engineering form since such radiative properties of water are not encountered in normal heat transfer problems. However, α_g can be estimated by using the equilibrium float program THERMNEW[6,9] to determine the absorptivity necessary to reproduce experimental flight gas temperatures. This procedure was applied to a variety of balloons and the required α_g was consistently found to be in the range of $0.0026 \le \alpha_g \le 0.0030$. Note that since this procedure is based upon experimental data, the resultant α_g values are independent of the actual contaminant. Further, based upon the small variation found for α_g, it is believed that good results can be obtained using a constant value.

As shown by many investigations,[6] one of the primary factors affecting balloon trajectory and thermal performance is the radiative properties of the balloon film, i.e., absorptivity/emissivity, transmissivity, and reflectivity in both the i.r. and solar. Unfortunately, previous estimates[6] of these quantities have varied so widely that their application to performance analyses has been essentially worthless. Fortunately, NASA Langley[10] has recently conducted very accurate measurements of the radiative properties of several balloon films. Based upon these data, the following values have been used in the present study for the radiative properties of polyethylene: $\alpha_{wsol} = 0.001$, $\epsilon_w = 0.031$, $r_{wsol} = 0.114$, $r_w = 0.127$, $\tau_{wsol} = 0.885$, and $\tau_w = 0.842$. As will be seen, the use of these values consistently leads to excellent temperature predictions.

Finally, based upon these measurements, it should be noted that the solar absorptivity of balloon film is extremely small. As a consequence, solar heating, either directly or via the albedo effect, will only slightly affect the film temperature; and, thus, it is unlikely that the daytime gas superheat is due to uneven solar heating of the balloon film. In other words, since the day-night i.r. heating is the same, these measurements verify that the daytime temperature enhancement of both the gas and the skin must be due to solar absorption in the lifting gas and subsequent heat transfer to the balloon film.

Balloon Drag Coefficient

As can be seen in Eq. (1), one of the primary forces acting on a balloon is drag; and to predict this force correctly, an accurate knowledge of the appropriate drag coefficient variation is required. Unfortunately, most wind tunnel tests on balloon shapes, such as Ref. 11, are for tethered balloons in which the freestream is horizontal and not vertical as in the present problem. Consequently, previous investigators have resorted to using an equivalent sphere model for which

$$D = \tfrac{1}{2}\rho\left|\frac{dz}{dt}\right|\frac{dz}{dt}C_D A \quad (17)$$

where A is cross-sectional area of an equivalent volume sphere, i.e.,

$$A=\pi\bar{R}^2 \tag{18}$$

and C_D is the drag coefficient for a sphere. Since sphere data are available and since over much of the flight profile the balloon shape is close to a sphere, this approach is also used in the present investigation.

Unfortunately, there exists disagreement in the literature as to the appropriate sphere values to use for balloons. Figure 1 plots sphere C_D over the Reynolds number range normally encountered during ascent. Here

$$Re=\rho_a\left|\frac{dz}{dt}\right|(2\bar{R})/\mu_a \tag{19}$$

The curve designated sphere is a representation of accepted smooth sphere values,[12] and it was used in the original version of Ref. 4. However, application of this correlation consistently led to high predictions for ascent rates below the tropopause in typical balloon flights. In this portion of the flight, a balloon typically encounters Reynolds numbers between 3×10^5 and 3×10^6.

As part of the present investigation, the effect of C_D on balloon ascent behavior was carefully studied; and it was determined that balloon ascent velocities between launch and the tropopause are very sensitive to the values of C_D. In fact, the present results agree with those of Kreith and Kreider in that the usual sphere value of about 0.1 is too low and that a value around 0.5 is more reasonable.

From an aerodynamicist's point of view the present required C_D variation with Reynolds number has the appearance of a flow characterized by a laminar rather than a turbulent separation. In 1935, Hoerner[13] performed drag measurements on smooth and rough spheres; and he found that on rough spheres the drag coefficient never had the laminar turbulent decrease typical of smooth spheres. In fact, he determined that C_D remained essentially constant at about 0.47 to 0.5 well up into the 10^6 Reynolds number range for rough spheres. He postulated that the boundary layer was separating laminarly and never reattaching. Today, it is known[14] from detailed tests and numerical studies, that on blunt-nosed airfoils the flow usually separates laminarly near the leading edge, transitions to turbulent flow above the resultant small separation bubble, reattaches, and then turbulently separates far downstream near the trailing edge. However, under certain low local Reynolds number conditions, the flow separates laminarly, transitions, but never reattaches. Thus Hoerner's explanation seems to be in agreement with both balloon and airfoil data; and thus the existence of an essentially constant drag coefficient over much of the flight regime of balloon appears reasonable. Apparently, a balloon behaves similarly to that of a rough sphere in a wind tunnel.

Unfortunately, there exists almost no experimental wind tunnel drag data for spheres at Reynolds numbers above 1×10^6. However, modern heavy lift balloons, which have float volumes greater than 5×10^5 m^3, have ascent Reynolds numbers significantly above 2.5×10^6 in the region between launch and the tropopause. Initial attempts to model such flights were unsuccessful in that they predicted excessive ascent velocities below the tropopause. Since these flights represented the only experimental data available for large spheres at large Reynolds numbers, these data[15] were used for the present model to estimate appropriate drag coefficients for $Re>2.5\times10^6$. Subsequent correlation yielded the curve shown on Fig. 1.

At first, the sharp increase in drag coefficient above 2.5×10^6 might seem unreasonable. However, during the early stages of ascent the shape of a large volume balloon is significantly different from that of a sphere. Thus the present

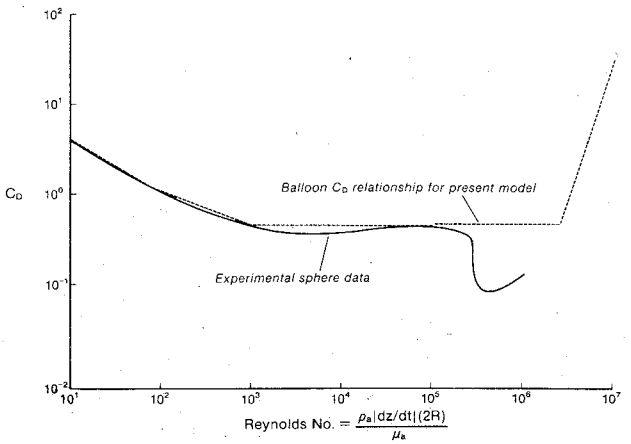

Fig. 1 Balloon drag coefficients.

large C_D values probably simply reflect the use of an equivalent sphere cross-sectional reference area in the formulation of drag and possibly the use of a value of ½ for the virtual mass coefficient C_m in Eq. (1). The effect of the latter was investigated for small- and medium-size balloons and found to be negligible. However, for large balloons, the effect of the virtual mass coefficient may be important and needs further investigation. Note that in the present model, the correlation shown is used whenever dz/dt is positive. When dz/dt is negative, the values are arbitrarily doubled.

Heat-Transfer Coefficients

For a balloon, the heat transfer between the film and the air can be either forced, which depends upon the velocity and character of the surrounding flowfield and occurs during ascent or descent, or natural, which occurs when the balloon is at rest or at very low velocity. While very little information exists for sphere- or balloon-like shapes in the regimes of interest for balloon flight, the present research indicates that the following are adequate: natural convection/film-air,

$$Nu=2+0.6(GrPr_a)^{1/4} \tag{20}$$

forced convection/film-air,

$$Nu=0.37(Re)^{0.6} \tag{21}$$

Here Nu is the Nusselt number, Gr is the Grashof number as usually defined, Pr_a is the Prandtl number of air (about 0.72), and Re is the same as Eq. (19). Equation (20) has the correct lower limit of 2 and is identical to that used by Kreith and Kreider.[1] Since it is only used at float conditions where convection is small compared to radiative effects, Eq. (20) should suffice.

Forced convection, however, is important in that it significantly affects the balloon film temperature during ascent. Equation (21) is the widely accepted form due to McAdams and reported by Kreith[16]; and it is based upon experimental data at $10<Re<10^5$, while modern large balloons have Reynolds numbers during ascent in the range 10^5-10^7. For small balloons, the results of the present research indicate that Eq. (21) is adequate. However, for large systems (maximum volumes above 5.38×10^5 m^3), it appears to underpredict the film-air heat transfer. Since balloon flight tests represent the only available data for large spheres, flight trajectory data have been used to deduce the applicable coefficient form. Thus, in the present model, for balloons having maximum volumes greater than 5.38×10^5 m^3, Eq. (21) is replaced by

$$Nu=0.74(Re)^{0.6} \tag{22}$$

The factor of 2 increase is strictly empirical and is justified by the fact that its application yields predictions in agreement with flight test data. Obviously, it is an area which requires further research. For convection inside the balloon, the following gas-film Nusselt number correlations have been used:

$$Nu = 2.5[2 + 0.6\,(GrPr_g)^{1/4}] \qquad GrPr_g < 1.5 \times 10^8$$

$$= 0.325\,(GrPr_g)^{1/2} \qquad GrPr_g > 1.5 \times 10^8 \quad (23)$$

In Eqs. (23), the breakpoint has been chosen so as to yield a smooth transition between the two formulas.

Atmospheric Model and Blackball Model

In any model for balloon performance, the variation in atmospheric properties with altitude must be represented accurately since these properties directly affect balloon lift, drag, and heat transfer. Fortunately, the variation in ambient temperature with altitude is well behaved in that the lapse rate, dT/dz, is essentially constant over well-defined layers. As a result, by specifying the temperature at specific altitudes and assuming a constant lapse rate in between, the pressure at any altitude within a layer can be easily computed by integrating $dp_a = -\rho_a dz$ over appropriate limits defined for each layer of the atmosphere model with constant lapse rate.

Consequently, in an attempt to keep the present method as simple as possible, a four-segment temperature profile model has been developed and incorporated into the numerical method. Using this approach, the 1962 Standard Atmosphere or the seasonal profiles encountered at the major launch site at Palestine, Texas, can be accurately modeled. It should be noted that in general the standard atmosphere is a poor representation much of the year.

Finally, in the atmospheric model, air thermal conductivity is assumed constant; and air viscosity is computed via a cubic curve fit vs altitude. It is believed that these representations are adequate for balloon flights.

To date the most accurate and convenient method of representing the Earth-air i.r. radiative input to a balloon is via the blackball concept,[1] and this approach was used in Eqs. (9) and (10). Its application, however, requires an accurate representation of the blackball temperature T_{BB} vs altitude. Normally, T_{BB} decreases linearly from a launch value about 5.5 K below the ambient temperature to a value at the tropopause. Above the tropopause, T_{BB} is normally constant at 214.4 K on clear days and 194.4 K for overcast skies, since most of the radiative input is from below.

Nevertheless, present results indicate that ascent trajectories are sensitive to Earth-i.r. behavior and that significant anomalies from "standard profiles" can occur. Usually, such variations could be expected after a long heat wave and/or dry spell; and thus the numerical model has been modified to permit a four-segment blackball profile. This possibility and sensitivity, of course, poses difficulties to an individual trying to predict a flight in advance and must be suitably considered.

Cloud Simulation

From the earliest attempts to analyze high-altitude balloon performance, it has been recognized that the presence of clouds significantly affects balloon behavior. Basically, the presence of clouds below a balloon reflects sunlight back to the balloon, thus increasing the solar input, and absorbs part of the Earth-air i.r. radiation. While clouds also radiate i.r. energy, they do so at a characteristic temperature lower than that of the Earth, and so the total effect of clouds is to reduce the i.r. radiative input to the balloon system while increasing the solar input. The combined effects may lead to either a daytime heating or cooling of the balloon, depending upon the relative radiative properties of the balloon film and gas. At night, clouds always cause a temperature decrease owing to the lowering of the i.r. input.

An analysis of various studies indicates that the type of clouds strongly influences the resultant behavior. A thick, low overcast will have a high albedo which may overcome the decrease in i.r. radiation and lead to increased balloon temperature. High clouds, such as thin cirrus, which may not even be visible from the ground have, however, a low albedo. They may, thus, only serve to decrease the i.r. input to the balloon and lead to a decrease in temperatures and subsequent descent.

Based upon studies of several flights, the following correlations and values are recommended for use in the present model:

$$r_e = 0.18 + 0.0039\,(\%\text{ cloud cover}) \quad (24)$$

Since the solar absorptivity of polyethylene balloon film is extremely low, the albedo effect on the film will be minimal; and Eq. (24) probably can be used for all types of clouds. However, for thin cirrus, an r_e of 0.18 is still suggested.

The blackball temperature above tropopause, for low-altitude and/or thick clouds, is

$$T_{BB} = 214.4\text{-}0.20\,(\%\text{ cloud cover}) \quad (25)$$

for thin high cirrus,

$$T_{BB} = 204.4\text{ K} \quad (26)$$

Gas Expulsion, Valving, and Ballasting

Owing to environmental conditions and operational requirements, a balloon may undergo gas expulsion, valving, and/or ballasting during the course of its flight. Gas expulsion, sometimes called burping, occurs whenever the balloon is at its maximum volume and continues to ascend owing to inertia and momentum. Since a zero-pressure balloon is always launched with excess free lift and hence gas, this phenomenon almost always occurs as the balloon goes into float. It can also take place if the balloon is at its maximum volume and the gas is subsequently heated, say, owing to sunrise. In the present model, gas expulsion is included.

Since in many flights operational specifications may also require an increase or decrease in ascent or descent velocities, the model also permits arbitrary gas valving and ballasting. Approximately 12 valvings and 50 ballast drops of arbitrary length and mass rate (g/min) can be treated with the present program configuration.

Tests with the method indicate that valving and ballasting must be accurately represented if a flight is to be correctly simulated.

Solution Method

An item of importance in the solution of a set of differential equations is the method of solution. Such a method should be simple, straightforward, and easily understood by a potential user; and yet it should be accurate and stable. Consequently, the standard Runge-Kutta method of order 4 has been used in the present program. This well-known method works well for nonlinear initial value systems of ordinary differential equations and only has an error proportional to the time step to the fourth power.

Obviously, the successful application of such a method requires the use of a sufficiently small time step. Unfortunately, the balloon problem is characterized by several high gradient regions where the variables are changing rapidly, such as ascent, sunrise, and sunset, and some low gradient periods, such as night float. A time step adequate for one region would be either computationally inefficient or inaccurate in the other. Thus the present model uses a variable time step dependent upon the current conditions.

Rigorous numerical studies with the present program and others indicate that the best approach to controlling the time

step is to place limits on the maximum change each major dependent variable can have over a time step. Based upon such studies conducted with the present code for realistic flight cases, the following limits have been selected: $|\Delta T_g|_{max} < 1$ K, $|\Delta T_f|_{max} < 1$ K, $|\Delta z|_{max} < 50$ m, and $|\Delta(dz/dt)|_{max} < 25$ m/min.

Another item of concern in any numerical solution is the possible error associated with cumulative significant digit and round-off error. Several double-precision (16 digits) arithmetic simulations have been performed and compared to their single-precision counterparts. In addition, several runs were obtained using maximum time steps of about 1 s. In all cases, the differences in results were insignificant.

Possibly the most important parameter affecting the ascent trajectory of a balloon is the initial mass of gas. Initial attempts to simulate actual flights with the present model were unsatisfactory in that the predicted ascent velocities above the tropopause were too low. Subsequently, a sensitivity analysis was conducted to determine which parameters affect this region; and it was determined that the most important quantity was the amount of lifting gas.

This analysis also showed that an initial mass of gas approximately 3% higher than that determined from the assumed initial free lift would yield computed flight trajectories in good agreement with measured trajectories. Possible explanations for this required added mass might be either that the actual mass of gas supplied at launch is consistently greater than that computed by the operations personnel or perhaps that the coefficient of virtual mass of ½ used in Eq. (1) is not correct for the balloon configuration. Further research is needed in order to explain fully the added mass requirement in the theoretical model. Nevertheless, all the flight simulations presented in this paper have assumed a coefficient of virtual mass of ½, corresponding to a sphere, and an initial mass of gas 3% greater than that computed from the free lift at launch.

Typical Results

Obviously, the primary objective of the present program is to develop a model and computer code capable of accurately analyzing the thermal and trajectory performance of a balloon flight. On July 24, 1980, engineering personnel of the National Scientific Balloon Facility flew RAD IV. This 66,375-m^3 balloon, flight number 167N, was launched during the daylight at about 1135 CDT, flew through sunset, and was terminated near sunrise the next morning. It was probably the most extensively instrumented, from a thermal viewpoint, flight to date. The balloon contained five gas thermistors suspended vertically along the centerline plus two others located 14 m outboard on the equatorial plane. In addition, it included ten film thermistors on the outside of the film and two on the inside.

Consequently, this flight has been analyzed with the present program using the model, heat-transfer and drag coefficients, parameter correlations, etc., developed in the present research effort. It is believed that by comparing these results with the flight data and those obtained using the old model (no gas radiation effects), an idea of the validity and accuracy of the present method can be obtained.

In comparing theoretical and experimental balloon trajectories, atmospheric pressure vs time should be used rather than geopotential altitude, since pressure is the quantity actually measured in an instrumented flight. This approach eliminates discrepancies which may result when an altitude is determined from a measured pressure and the 1962 Standard Atmosphere and the actual altitude profile differs from the standard. On all pressure plots in this paper, the vertical scale is $\log_e(P_{launch}/P_a)$. Since the atmosphere is almost exponential in nature, such a scale yields curves which look similar to an altitude plot.

Figures 2a and 2b compare the present pressure trajectory predictions with the flight data and predictions using the old

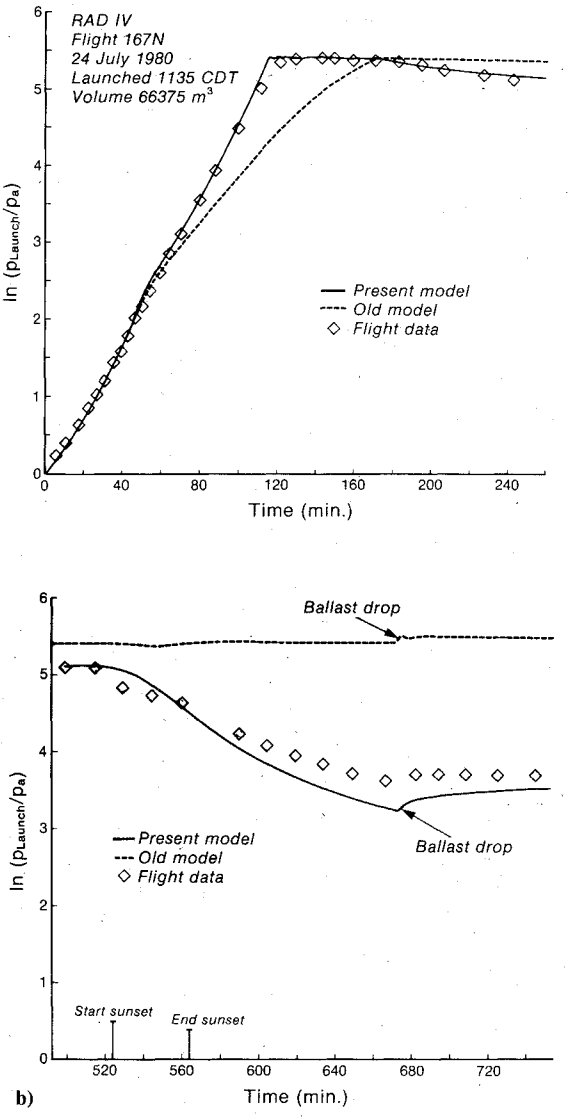

Fig. 2 Pressure altitude trajectories for RAD IV.

model. The agreement between the flight data and the present theory is generally excellent.

It should be noted that upon arrival at float, the present theory shows that the balloon went through several vertical oscillations in the process of expelling or "burping" gas before settling down to a steady float altitude. In addition, the effect of the balloon passing over high cirrus clouds at 170 min can be seen in the onset of a gentle descent; and the new model correctly predicts the trend of this effect.

However, probably the most interesting of these plots is Fig. 2b, which shows the trajectory during sunset. While not exactly accurate, the predicted trajectory from the new model has the correct behavior. During the latter portion of sunset, the descent velocity is quite high, reaching −137 m/min, followed by an asymptotic decrease in descent rate during the night. At 673 min, a 22.64-kg ballast drop was executed in order to stop the descent. At this point, the descent velocity according to the theoretical model was still −43 m/min.

As can be seen on Fig. 2b, this ballasting did stop the descent and result in an essentially stable float for the rest of the night in both the flight and theoretical cases.

Figures 3a and 3b show temperature profile comparisons for RAD IV. Due to the fact that flight 167N was launched remotely, completely accurate thermistor data were not obtained prior to about 80 min into the flight; and the plotted experimental data represent the average of all pertinent thermistor readings. In general, the predicted temperatures

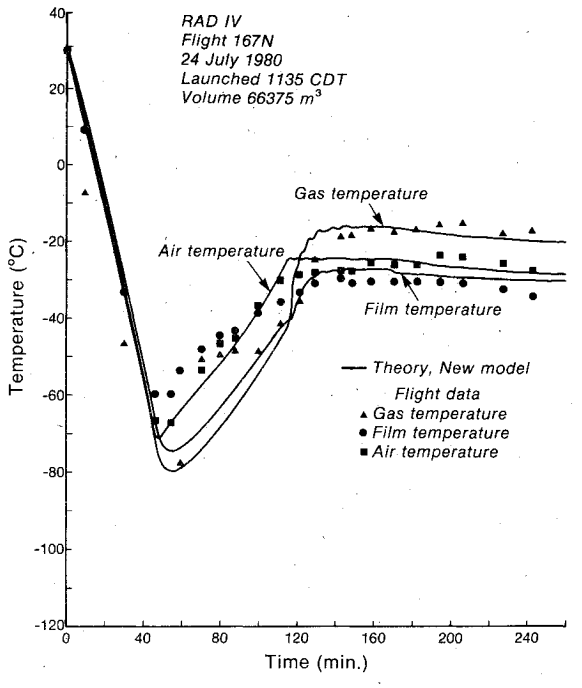

a)

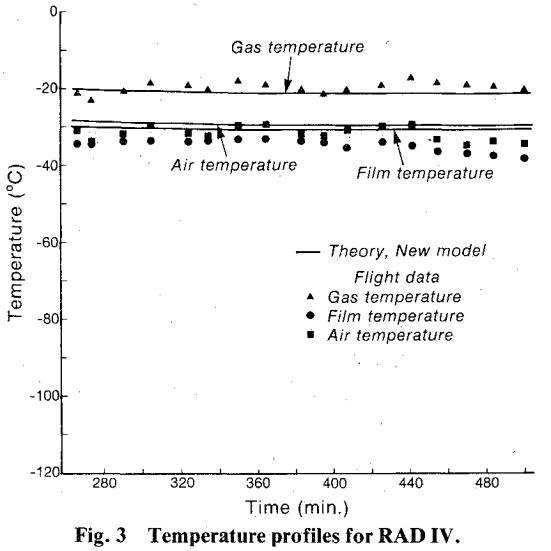

b)

Fig. 3 Temperature profiles for RAD IV.

are in acceptable agreement with the flight data, particularly during the daytime float portion of the flight. There (Fig. 3b) the gas temperatures are accurately predicted; and the relationship between gas, ambient, and film values, with the gas highest and film coolest, is correctly reproduced.

While these results indicate that the present method is reasonably accurate, they do not demonstrate that it is an improvement over previous models[1] which assume that the lifting gas is radiatively inactive. This situation can be duplicated in the present model simply by setting α_g and ϵ_g equal to zero. Results for such an assumption are shown for RAD IV on Figs. 2 and 4, and they should be similar to those which would be obtained using the method and code of Ref. 1. As can be seen on Fig. 2a, the resultant pressure trajectory is in good agreement with flight data up to the tropopause. Above this altitude, however, the radiatively inactive model is in serious error and significantly mispredicts the time to float. In addition, as shown on Fig. 2b, the old thermal model completely misses the actual flight behavior during and after sunset. This absence of an altitude decrease is due to the fact that the solar absorptivity of polyethylene is very small and thus it is relatively insensitive to the presence or absence of sunlight.

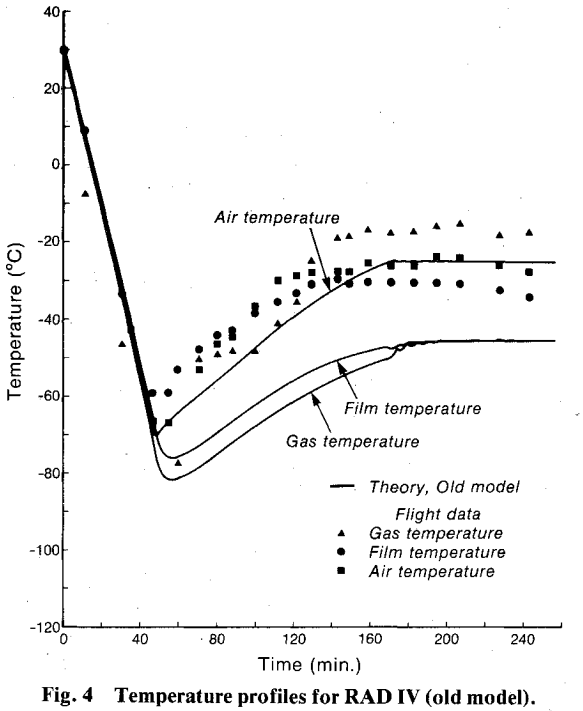

Fig. 4 Temperature profiles for RAD IV (old model).

Temperature profiles for the radiatively inactive case are portrayed on Fig. 4, and they also show very poor agreement with the flight data. During daytime float, the gas and film temperatures predicted by this old approach are on the order of 20°C too cold, and the variation during sunset is not even close to the actual behavior.

Based upon the comparison of Figs. 2a, 2b, and 3a with Fig. 4, it is obvious that the present thermal model is a significant improvement over previous formulations. In addition, based upon these results and those for several flights,[17] it is believed that the present method and code is a valid model for high-altitude balloon flight. It should, with correct use, yield accurate thermal and trajectory information suitable for analyzing and predicting the behavior of scientific balloons.

Conclusion

A trajectory and thermal model for balloon performance has been developed which accounts for the experimentally observed gas temperature enhancement. It has been concluded that the most likely explanation for the observed gas thermal behavior is water vapor contamination, although there is currently no direct proof. Consequently, the gas absorptivity has been deduced from equilibrium float measurements, and its emissivity has been estimated from water vapor radiation theory. In addition, it has been determined that drag coefficients strongly affect trajectories below the tropopause, that the mass of gas strongly affects performance above the tropopause, and that forced convection significantly affects large-volume balloons. In all cases, it has been found that the Earth-air blackball temperature variation is very important. Areas requiring further research are drag coefficients for realistic shapes typical of balloons, determination of the actual cause of the gas temperature enhancement, and good experimental values for forced convection coefficients in the balloon flight regime.

It is believed that the present project has yielded a theoretical model and computer program that will permit better predictions of balloon temperatures and trajectories and which will lead to a better understanding of overall balloon behavior. Such predictions and analyses can be used to provide better input data for advanced structural analysis methods and for studies of ballast management and balloon performance optimization.

Acknowledgments

This research was primarily supported by the National Aeronautics and Space Administration, Wallops Flight Center, Wallops Island, Va., under Contract NAS6-3072. The technical monitor for this work was Harvey Needleman of the Sounding Rocket Program Office, LTA Branch, of NASA Wallops. Partial support in the form of salaries and computer funds was also provided by the Aerospace Engineering Division of the Texas Engineering Experiment Station. The authors also wish to express their appreciation to the staff of the NASA Wallops, LTA Branch, and to the members of the Engineering Department, NSBF, Palestine, Texas, for the provision of flight data and their helpful discussions and advice; and to L.G. Clark and C.C. Kiser of NASA Langley for providing balloon film radiative property data.

References

[1]Kreith, F. and Kreider, J.F., "Numerical Prediction of the Performance of High Altitude Balloons," NCAR Technical Note NCAR-IN/STR-65, Feb. 1974.

[2]Kreider, J.F., "Mathematical Modeling of High Altitude Balloon Performance," AIAA Paper 75-1385, 1975.

[3]Lucas, R.M. and Hall, G.H., "The Measurement of High Altitude Balloon Gas Temperature," *Proceedings of the 4th AFCRL Scientific Balloon Symposium*, edited by J.F. Dwyer, 1967, pp. 279-293.

[4]Lucas, R.M. and Hall, G.H., "The Measurement of Balloon Flight Temperatures through Sunset and Sunrise," *Proceedings of the 5th AFCRL Scientific Balloon Symposium*, 1968, pp. 121-130.

[5]Lucas, R.M., Hall, G.H., and Allen, B.M., "Experimental Balloon Gas and Film Temperatures," *Proceedings of the 6th AFCRL Scientific Balloon Symposium,* edited by L.A. Grass, 1970, pp. 227-241.

[6]Carlson, L.A., "A New Thermal Analysis Model for High Altitude Balloons," *Proceedings of the 10th AFGL Scientific Balloon Symposium*, edited by C.L. Rice, March 1979, pp. 187-206.

[7]Kreith, F., *Principles of Heat Transfer*, 3rd. ed., Harper & Row, New York, 1973, pp. 219-308.

[8]Herzberg, G., *Atomic Spectra and Atomic Structure*, Dover, New York, 1944, pp. 64-66.

[9]Carlson, L.A., "THERMNEW—A Preliminary Model and Computer Program for Predicting Balloon Temperatures at Float," Texas Engineering Experiment Station Report 921CI-79101, Oct. 1979.

[10]Kiser, C.C., "Balloon Material Testing for Texas A&M University," Unnumbered Memo to TAMU from NASA/LRC, Feb. 26, 1980.

[11]Sherburne, P.A., "Wind Tunnel Test of Natural Shape Balloon Model," *Proceedings of the 5th AFCRL Scientific Balloon Symposium,* March 1968.

[12]Schlichting, H., *Boundary Layer Theory*, 6th ed., McGraw-Hill, New York, 1968, pp. 17-19.

[13]Hoerner, S., "Tests of Spheres with Reference to Reynolds Number, Turbulence, and Surface Roughness," NACA-TM-777, Oct. 1935.

[14]Carlson, L.A., "A Direct-Inverse Technique for Low Speed High Lift Airfoil Flowfield Analysis," AGARD-CP291, Oct. 1980, pp. 26-1-26-10.

[15]Hilditch, S.F., "Balloon Flight 1116P Data Reduction," Report from Computer Sciences Corporation to NASA Wallops, Nov. 1979.

[16]Kreith, F., *Principles of Heat Transfer*, 3rd ed., Harper & Row, New York, 1973, pp. 471-473.

[17]Carlson, L.A. and Horn, W.J., "A Unified Thermal and Vertical Trajectory Model for the Prediction of High Altitude Balloon Performance," Texas Engineering Experiment Station Report TAMRF-4217-81-01, June 1981.